Earthquakes and Structures, *Vol. 9, No. 1 (2015) 195-219*
DOI: http://dx.doi.org/10.12989/eas.2015.9.1.195

Establishing optimal gap size for precast beam bridges with a buffer-gap-elastomeric bearings system

Mousa M.N. Farag[a], Sameh S.F. Mehanny[*] and Mourad M. Bakhoum[b]

Department of Structural Engineering, Faculty of Engineering, Cairo University, Gamaa Road, Giza, Egypt

(Received August 19, 2014, Revised December 10, 2014, Accepted May 6, 2015)

Abstract. A partial (hybrid) seismic isolation scheme for precast girder bridges in the form of a "buffer-gap-elastomeric bearings" system has been endorsed in the literature as an efficient seismic design system. However, no guides exist to detail an optimal gap size for different configurations. A numerical study is established herein for different scenarios according to Euro code seismic requirements in order to develop guidelines for the selection of optimal buffer-gap arrangements for various design cases. Various schemes are hence designed for ductile and limited ductility behavior of the bridge piers for different seismic demand levels. Seven real ground records are selected to perform incremental dynamic analysis of the bridges up to failure. Bridges with typical short and high piers are studied; and different values of initial gaps at piers are also investigated varying from a zero gap (i.e., fully locked) condition up to an initial gap at piers that is three quarters the gap left at abutments. Among the main conclusions is that the as-built initial gaps at piers (and especially large gap sizes that are ≥1/2 as-built gaps at abutments) do not practically reduce the seismic design demand and do not affect the reserve capacity of the bridge against failure for bridges featuring long piers, especially when these bridges are designed a priori for ductile behavior. To the contrary, the "buffer-gap-elastomeric bearings" system is more effective for the bridge schemes with short piers having a large difference between the stiffness of the bearings and that of their supporting (much stiffer) squat piers, particularly for designs with limited ductility. Such effectiveness is even amplified for the case of larger initial as-built gap sizes at piers.

Keywords: buffer; gap; elastomeric bearings; seismic response; EC8

1. Introduction

Bridge damage due to earthquakes can cause significant disruption to the transportation system, resulting in substantial direct and indirect losses (Stefanidou and Kappos 2013). Some past earthquakes have resulted in large horizontal displacements of the superstructure (i.e., deck) that have led to unseating of bridge spans and unexpected large straining demands that damaged critical components of the bridge such as elastomeric bearings. As a solution to address the vulnerability of bridge bearings and other critical components, one or more of many special

*Corresponding author, Professor, E-mail: sameh.mehanny@stanfordalumni.org
[a]E-mail: mousa.maher@yahoo.com
[b]Professor, E-mail: bakhoumm@gmail.com

http://www.techno-press.org/journals/eas&subpage=7 ISSN: 2092-7614 (Print), 2092-7622 (Online)

features/devices may be introduced at the bridge superstructure-substructure junction that could control the large displacement of decks. These may be in the form of restrainer cables, high strength bar restrainers, bumper blocks, shear keys, keeper brackets, steel pipe restrainers, etc. and they hence serve as seismic isolation means.

Seismic isolation of bridges is considered as a competitive solution to reduce seismic demand and hence improve bridge response under seismic excitations. Seismic isolation exhibits a breakthrough in contemporary bridge engineering (Mitoulis 2013). The principal of isolation is to protect the bridge piers, by either reducing their seismic actions or through the increase in the damping of the structure. A revolution of seismic isolation in bridge engineering is established during the last decades. To date there are several hundred bridges in the United States, New Zealand, Japan and Italy using seismic isolation principles and technology for their seismic design (Buckle *et al*. 2006). An isolation system placed between the bridge superstructure and its supporting substructure, through for instance the inclusion of elastomeric bearings, lengthens the fundamental period of the bridge structure with the deck actually longitudinally "floating" along the isolation "pier-deck" interface. This lengthening of the fundamental period of vibration helps that the bridge does not respond to the most damaging energy content of the earthquake input (Kunde and Jangid 2006), while offering damping to the bridge. The bridge designer is given the choice between commercially available bearings or any other, experimentally tested, rubber bearings suitable for seismic isolation. During the bridge service, bearings shall accommodate the constraint movements of the deck that are the changes in the length of the bridge due to thermal effects, creep, shrinkage, and prestressing.

However, there are bridges in which the seismic loading of piers is not effectively reduced when using classic seismic isolation exclusively through elastomeric bearings and the like. The ineffectiveness of seismic isolation with typical elastomeric bearings was particularly observed in bridges with tall piers. During the last years many bridge engineers and academics have therefore shed light on alternative variation to classic seismic isolation. "Partial" or "hybrid" bridge isolation schemes hence emerged to reduce deck displacements (Bandyopadhyay *et al*. 2010, Monzon *et al*. 2012) and accordingly decrease required ductility demands in the supporting piers. Hybrid seismic isolation has been found to offer lower levels of damage and negligible residual deformations after seismic events. A typical example of a "hybrid" seismic isolation system that provides both viable and efficient solution for an improved seismic performance of bridges is the use of shear keys/buffers that restrict longitudinal deck displacements at piers. Use of shear keys is a mature and reliable technology covered extensively by both the current state of the art and codes. External shear keys have been proposed in bridges to minimize longitudinal movements (Mitoulis and Tegos 2010). For instance, Dicleli (2002) found that the hybrid seismic isolation system provided a structure with a fundamental period long enough to attract smaller seismic forces, while controlling the magnitude of bearings' displacements. It also resulted in a more uniform distribution of seismic forces among substructure elements, while the piers may provide a restoring force to re-center the structure in such circumstances. Hindi and Dicleli (2006) studied the modification of the seismic response of bridges when modifying the fixity conditions of bearings. Bridge systems were modified to obtain different configurations of bridge earthquake resisting systems. Their research yielded that changing the fixities of the bearings may be an effective response modification technique to mitigate the effect of seismic forces on vulnerable substructures of the bridge under consideration. As per Mitoulis (2013), AASHTO (2002), Caltrans (1999) require the use of shear keys/buffers to minimize the possibility of span unseating. Accordingly, Euro code EN 1998-2 (2005) requires the use of seismically inactive shear keys that

reduce the deck dislodgment potential, while additional to this the Japanese code JRA 1997 & 2002 explicitly requires stoppers to provide means to dissipate the seismic energy. The Chinese code specifies that, except for displacement limiting and dissipation, shear keys can be used for two levels of resistance (Wang *et al*. 2012).

2. Problem statement

Bridges consisting of precast (i.e., prefabricated) beams investigated in this research are largely adopted worldwide (North Africa, Middle East, Europe, Gulf Area, etc.) due to the construction speed of the bridge deck and the cost savings gained when utilizing this type of construction. In these precast girder bridges, introducing on-site gaps between (a) precast beams' ends resting on inverted tee pier's cross-heads (i.e., cap beams) through elastomeric bearings on one hand and (b) adjacent face of the inverted stem of these cap beams (serving as seismic buffers in the longitudinal direction) on the other hand, is confirmed to reduce the forces transmitted to the piers and foundations at the design level earthquake (Ayoub and Helmy 2000). An ideal situation is to keep both the deck displacement and the force in column in safe level under design level earthquakes. While the two expectations may be seemingly contradictory, the effectiveness of this "buffer-gap-elastomeric bearings" system in achieving such dual-goal depends on lateral resistance it can provide, and balancing acts can be made to find a solution to effectively control deck displacement and maintain integrity of bridges. Pounding is however expected at the instant when the gap between deck component and seismic longitudinal buffer closes.

As previously highlighted in the literature, seismic isolation of bridges is a very effective way of protecting bridges from the damaging effects of earthquakes in seismically active regions. Note that in practice isolated bridges using elastomeric bearings (an effective passive method for reducing earthquake-induced forces) when equipped with seismic buffers are considered as partially/hybridly-isolated systems that combine the beneficial period lengthening at the design seismic demand due to elastomeric bearings with a scheme that controls displacement demand at levels higher than the design demand level up to complete collapse. The present research sheds the light on the effectiveness of such partially-isolated systems for the benefit of bridge engineers and academics. It is questionable though whether this hybrid "buffer-gap-elastomeric bearings" system will respond as prescribed through design, or if bridges will still require retrofitting after frequent earthquakes larger than the design level. In the hybrid system described in this paper, the gap is selected in such a way that the elastomeric bearings are free to laterally deform under ambient (thermal loads, pre-stress, creep, shrinkage, etc.) or traffic loads, while the precast beams impact on the buffers (i.e., cross-heads or cap beams) only under moderate or strong earthquake loads. Activation of the seismic buffers (involving the "cap beam-pier" system) due to impact results in sudden increase of the stiffness of the structure. In common design practice, the gaps in the bridge longitudinal direction between the buffers and the deck-bearing system are usually selected such that the impact with the buffers occurs before the pier yielding (Psycharis and Mageirou 2003).

To recap, the deformations of elastomeric bearings under seismic forces are usually very large. The designer has therefore the option of either using special seismic elastomeric bearings that can withstand these displacements without damage or rupture - and accordingly adopts in his design a pure longitudinally "floating" deck restrained only at the abutments' back-wall (a sacrificial/fuse back-wall), or instead providing seismic restrainers (i.e., buffers) to control such displacements of the bearings. In the presence of buffers, and in order to allow for longitudinal thermal movements

and other permanent and quasi-permanent displacements as well as a portion of anticipated seismic displacement for possible energy dissipation, the buffers - in our case the stem of the inverted tee cap beam at top of piers - are placed with a calculated clearance (gap) from the end of the precast beam resting on the elastomeric bearing. This gap along with the buffer serves as a seismic link proposed by recent seismic provisions and standards EN 1998-2 (2005) worldwide to cater for some energy dissipation mechanism before full locking between the bridge deck and the substructure. This gap however introduces nonlinearity in the seismic response of the bridge and, therefore, is sometimes ignored by bridge engineers throughout the design process for the sake of simplicity which may have non-conservative implications on the response thereafter.

3. Research significance

Buffer-gap-elastomeric bearings system for real-world precast beam bridges has been previously introduced and confirmed (Ayoub and Helmy 2000, Psycharis and Mageirou 2003) as a competitive seismic design scheme. Nonetheless, optimal gap sizes for various design scenarios have not been established since these pioneering efforts. The core target of the present research is hence not only to meticulously investigate the merits of the presence on site of initial (preset) gaps at piers along with a buffer/stopper system, but also to determine appropriate sizes for such gaps to *effectively* reduce the seismic design demand transmitted to the substructure elements and to enhance reserve capacity against failure whenever possible. The research assesses if introducing a specific initial gap size is effective (and offers a positive demand-reducing means), or instead unfavorable and not capable of reducing the seismic demand at a seismic event corresponding to the design level earthquake when compared to the seismic demand acquired by the same bridge that is instead not only initially designed but also constructed for the fully locked condition (i.e., with zero gap). Likewise, and using the same rationale, the paper examines whether introducing an initial gap to the "buffer-elastomeric bearings" system serving as a hybrid isolation scheme to bridges of this type adds to the overstrength (i.e., reserve capacity against collapse) of a bridge already designed and constructed for the fully locked condition, or conversely reduces such inherent overstrength. This definitely depends on the relative and mutual effects of the following factors: (1) the size of the gap at various supports, (2) the shear stiffness of the elastomeric bearings, (3) the height and cross-section (and hence flexibility) of the supporting piers, (4) the design of these piers being performed *a priori* for limited ductility or ductile behavior, etc. The present research finally inspects whether the usually adopted design approach of dimensioning piers and their reinforcement for a zero gap situation, i.e., for the fully locked condition (or sometimes called "hinged-structure" as per Psycharis and Mageirou (2003)) is beneficial or not to the actual seismic response up to collapse limit state of the bridge typically equipped on-site with a specific gap at piers and abutments to cater for thermal and other lateral (non-seismic) loading. In other words, does this simplified design approach for the fully locked condition, albeit the actual presence of the gap on site, provide a more conservative design scheme that warrants the bridge a reserve capacity (or overstrength) against collapse? Note that this design approach is often adopted in design firms worldwide for its simplicity and endorsed for its practicality despite the ad-hoc and debatable pre-assumption of its ultimate conservatism from a design perspective.

In the present research, the impact (i.e., pounding/shock) effects between the deck's precast beams and the pier's cap beam during the engagement of the seismic buffers is not considered. In some cases, as highlighted in the literature, this impact may lead to higher than expected ductility

demand in the piers (Psycharis and Mageirou 2003). Pounding (or impact) may accordingly cause some potential threats to bridge structures. However, there are as well some advantages that can be provided by pounding. Some researchers have for instance suggested that pounding generally reduces the response of bridge frames because of the energy dissipated during pounding and because pounding disrupts the buildup of resonance (DesRoches and Muthukumar 2002). Moreover, as extra precaution in moderate to high seismic zones, the seismic buffers are usually equipped with vertical rubber pads that are mounted on their surface to reduce (and damp) any damaging shock effects - as requested in EN 1998-2 (2005) - that may arise from the pounding of the deck with the substructure at the instant of gap closure.

4. Design and modeling of the case study bridge

4.1 Bridge description

The case study bridge is a continuous 3-span bridge as shown in Fig. 1. Each span consists of simply supported precast pre-stressed concrete beams resting on elastomeric bearings on top of reinforced concrete inverted tee cap beam atop of the pier. The deck continuity is imposed through a top reinforced concrete "connecting" slab above precast beams running continuous above piers. The bridge is 84 meters-long divided into three equal spans 28 meters-long each, and is supported on two abutments at its two ends. The bridge is straight in plan, and all piers are perpendicular to the bridge deck center line. The bridge deck consists of 10 precast pre-stressed beams covered by a 200 mm-thick top RC slab. The precast beams are resting on top of a cap beam at piers location, and on top of abutment's shelf through elastomeric bearings. Pier cross section dimensions and reinforcement are presented in what follows according to various adopted design scenarios.

The role of the top RC connecting slab is to ensure the axial continuity (i.e., diaphragm action) of the bridge deck across adjacent spans. This continuity accordingly prohibits any out-of-phase movement of the adjacent decks in the longitudinal direction during shaking. It further avoids the use of expansion joints at pier locations which improves the riding comfort. It is noted from Fig.1 - Detail 1 that this connecting "continuity" slab is not resting on the inverted cap beam. It is instead spanning between the adjacent precast beam decks hence also providing continuity under the vertical live loading but with reduced hogging bending moment at the ends of precast beams due to its much smaller flexural stiffness relative to that of the noticeably thicker "precast beam-slab" deck. Precast beams carry their own weight and overtopping slab weight as simply supported beams before casting this connecting/continuity slab that is typically cast at a later stage after installation of beams and after casting of overtopping slab, while they carry superimposed dead loads and live loads with some continuity effects after casting the connecting slab. Finally, it is to be noted that the horizontal force due to the deck inertial effects during shaking is transferred from the deck to the pier entirely through the elastomeric bearings before locking, i.e., before activation of the buffer; then, when locking occurs, the force is transmitted to the pier shaft across the whole surface of contact between the precast beams' ends and the adjacent face of the web of the inverted cap beam.

4.2 Modeling using OpenSees

The structural analysis platform OpenSees (2009) is used to determine structural response of

the case study bridge. The concrete material used is Concrete01 material as defined in OpenSees manual. This material is the uniaxial Kent-Scott-Park (Scott *et al*. 1982) concrete material object with degraded linear unloading/reloading stiffness according to the work of Karsan and Jirsa (1969) and with no tensile strength. The calculation of the required data for defining the Concrete01 material is based on a set of semi-empirical equations considering the effect of confinement of the concrete section due to stirrups. This results in an increase in the piers concrete compressive cylinder strength of 28 MPa, and also an increase in the strain (both at the maximum compressive strength and at the concrete crushing strength). Stress and strain limits of the confined

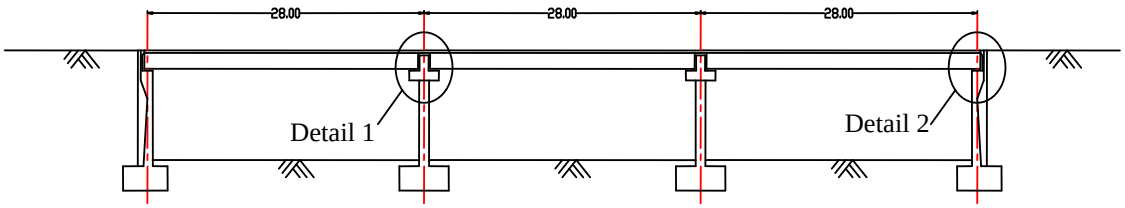

Elevation of the case the study bridge. (dimensions in m)

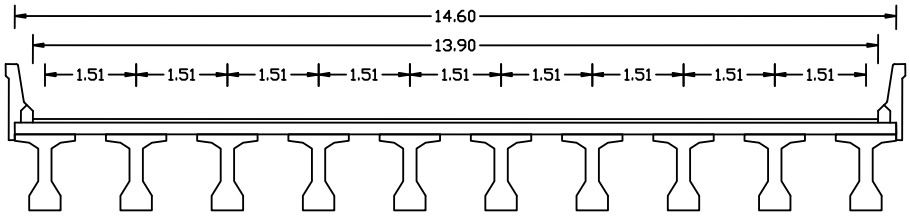

Deck cross-section. (dimensions in m)

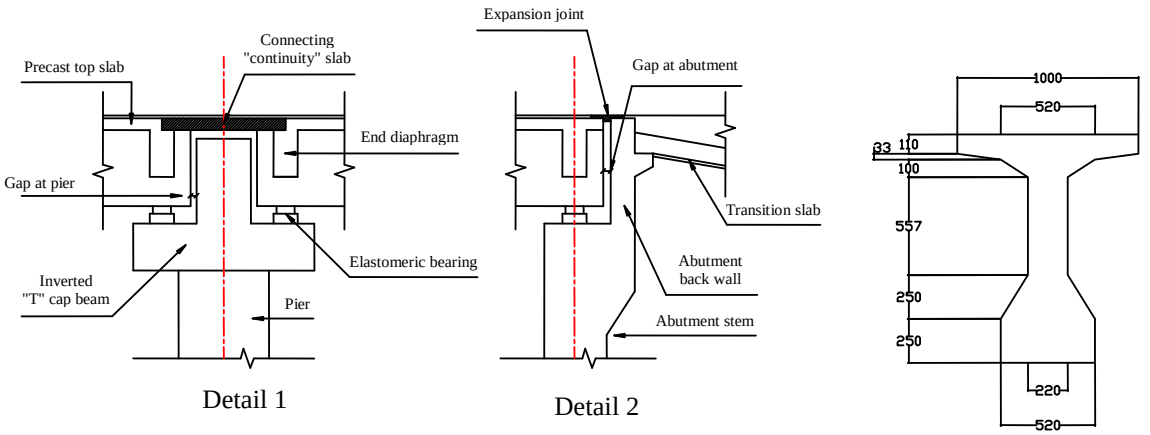

Detail 1

Detail 2

Precast beam
(dimensions in mm)

Fig. 1 Case study bridge elevation, deck and precast beams cross-sections and other standard details

and un-confined concrete materials are according to EN 1992-2 (2005) and are illustrated in Farag (2013). According to the above, the compressive strength of the confined area is 35 MPa, the strain at reaching the maximum strength of the confined area is 3‰ and the ultimate strain of the confined area is 14‰ for strict code detailing associated with ductile design; these values are different for detailing associated with limited ductility design (refer to Farag 2013). The steel material model used herein is Steel02 material as defined in OpenSees manual. This material is a uni-axial bilinear steel material object with kinematic hardening and optional isotropic hardening described by a non-linear evolution equation. Its behavior is characterized by an initial linearly elastic portion of the stress-strain relationship, with a modulus of elasticity Es=200 GPa, up to the yield stress fy, followed by a subsequent region of strain hardening. The yield stress of the reinforcing steel is 420 MPa and the hardening modulus is 4.2 MPa. For other parameters controlling the transition from elastic to plastic branches (refer to Farag 2013).

Distributed plasticity beam-column elements with a displacement-based formulation are adopted to model piers of the case study bridge. Such formulation approximates the displacement field within the element. In order for this type of formulation to accurately capture the concentration of plastification (and consequently high curvature gradients at plastic hinge locations), a relatively fine discretization of beam-column members should be maintained. Good results are expected for elements size approximately equal to the length of the plastic hinge. In the present research, two heights of bridge piers are investigated (namely, 7 and 14 m). In order to achieve high accuracy with adopted displacement-based element formulation, and after carrying out a sensitivity analysis (Farag 2013) to come up with the most convenient, reliable and accurate discretization of piers of the case study bridges, we ended up by subdividing the pier total height to a number of successive elements each with a maximum length not exceeding 1.4 m - roughly the anticipated plastic hinge length. As a result, piers that are 7 m high are divided into five elements and piers that are 14 m high are divided into ten elements. Each element features ten integration points. Piers are assumed fixed to their foundations at the bottom - i.e., soil-structure interaction is ignored. P-Delta transformation in OpenSees is also activated. The bridge deck is modeled using elastic frame elements as per EC8 recommendations which state that "the bridge deck shall remain within the elastic range under seismic loads" (EN 1998-2 2005). It should be noted that for pre-stressed concrete decks, the stiffness of the uncracked section is considered in modeling the deck (EN 1998-2 2005). Bridge masses are lumped at the level of the deck and are assigned in the direction of excitation of interest to the current research (longitudinal direction of the bridge). Lumped masses include dead loads in addition to 20% of the bridge live loads according to EC8. Bridge dead loads consist of bridge own weight, super imposed dead load (60 mm of asphalt) and barriers.

4.2.1 Elastomeric bearings and anticipated failure strain

Elastomeric bearings considered in this research are laminated rubber bearings consisting of rubber layers reinforced by integrally bonded steel plates. They are classified by EN 1998-2 (2005) as simple low-damping bearings with an equivalent viscous damping ratio ξ approximately equal to the global viscous damping of the structure (namely, 0.05 herein). Such bearings may be considered as linear elastic members, deforming in shear (and possibly in compression) with equivalent elastic stiffness in the horizontal direction equal to $G_b A_b/t_b$ where G_b is the shear modulus of the elastomer, A_b its effective horizontal area and t_b is the total thickness of the elastomer. The maximum shear strain resisted by elastomeric pads prior to failure is estimated at ±150% in Caltrans-SDC (2009). This value is believed to be fairly conservative for design

purposes. Experiments show that the elastomeric bridge bearings perform exceptionally, even under seismic loading conditions (Konstantinidis *et al*. 2009). The bearings were able to withstand very large shear strains without any damage, which reinforces the idea that present design guidelines for bridge bearings that hence limit the combined *design* shear strains under *service* loading to 50% may be overly conservative.

Experimental results further show that the roll-off response when the bearings are highly sheared is limited by the fact that the free edge of the bearing rotates from the vertical towards the horizontal with increasing shear displacement, and the limit of this process is reached when the originally vertical surfaces at each side come in contact with the horizontal surfaces at both top and bottom (i.e., roll-over). Further horizontal displacement beyond this point can only be achieved by slipping. Slip can produce damage to the bearing through tearing of the rubber, distortion of the reinforcing steel, and heat generated by the sliding motion. Thus the ultimate displacement for an un-bonded bearing of this type can be specified as that which transforms the vertical free edge to a horizontal plane. Determining analytically the ultimate shear strain is very complicated, but a lower bound of the ultimate shear strain can be obtained if certain assumptions are made as per Konstantinidis *et al*. (2009). It has been further noted there that only for the test with 300% imposed shear strain, for which sliding was observed, does the hysteretic loop shape change. It has been also stated that under shear loading of these simple low-damping steel-reinforced elastomeric bearings, the shear strain at failure can exceed 400%. Referring to another valuable very recent experimental investigation available in the literature, Manos *et al*. (2011) stated that strain amplitudes larger than 250% resulted in the debonding of the elastomer from the steel plating. According to the above, the shear strain limit anticipated at elastomeric bearings *actual* failure has been assumed to be 300% for all investigations in the current research. Better estimates for this "at-failure" shear strain could be considered in the future based on additional tests.

4.2.2 Modeling of "abutment-gap-elastomeric bearings" system

Abutments at both ends of the bridge are modeled in such a way to restrain the movement in the vertical direction while allowing rotation about an axis perpendicular to the bridge alignment. Translational movement in the longitudinal direction is also prevented via non-sliding elastomeric bearings. Non-sliding elastomeric bearings on abutment's shelf and passive earth pressure behind abutment are modeled using parallel material in OpenSees (i.e., two springs in parallel as shown in Fig. 2). The first is a material (or spring) to represent the bearings where a primarily elastic material is used, while the second spring/material is for modeling passive earth pressure behind abutment's back wall where elastic perfectly plastic material with "compression only" gap is considered (Caltrans-SDC 2009) as shown in Fig. 3. Horizontal spring (in the deck longitudinal direction) modeling the shear stiffness of an elastomeric bearing is assigned a stiffness value that is equal to the shear modulus of the elastomer material, G_b, multiplied by the foot print area of the bearing, A_b, and divided by the total thickness of the elastomer, t_b. The shear stiffness of elastomeric bearings at each end of precast beams represented by a single spine in the current computational model is hence the stiffness of a single bearing estimated as above multiplied by their number, n, which is simply the number of precast beams. As per EN 1998-2 (2005) - Cl. 7.5.2.4 (5), G_b has been taken in the present research with the value proposed for short term (i.e., seismic) response as 1.485 MPa (G_b=1.1×(1.15 MPa+0.2 MPa)). For 0.15 g design scenarios investigated in the current research, t_b=0.1 m, while for 0.3 g design scenarios t_b is taken equal to 0.15 m in order to accommodate anticipated shear deformation of the bearing under lateral seismic

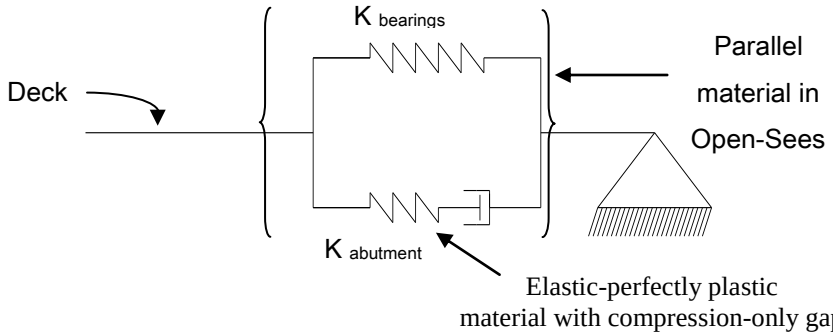

Fig. 2 Modeling of abutment with non-sliding bearings using "parallel material" feature in OpenSees software

design loading. Finally A_b has been taken equal to 0.25×0.35 m^2 for all design scenarios to adequately carry vertical loading.

On the other hand, the abutment stiffness is modeled as per Caltrans-SDC (2009) with its value calculated as $K_{abutment}$=11500.0 w (h/1.7); where w and h are the width and the height, respectively, of the back wall in meters. The width of the back wall is taken as the bridge deck width minus twice of the deck depth. $K_{abutment}$ is in kN/m (Aviram *et al*. 2008). The strength furnished by "abutment-embankment passive earth pressure" is estimated in kN using Caltrans-SDC (2009) recommendations: $P_{abutment}$=239.0 wxh (h/1.7). Schematic backbone curve of the "abutment-gap" system is shown in Fig. 3 for the case with 200 mm initial gap at abutment applicable to the 0.3 g design scheme as will be clarified later.

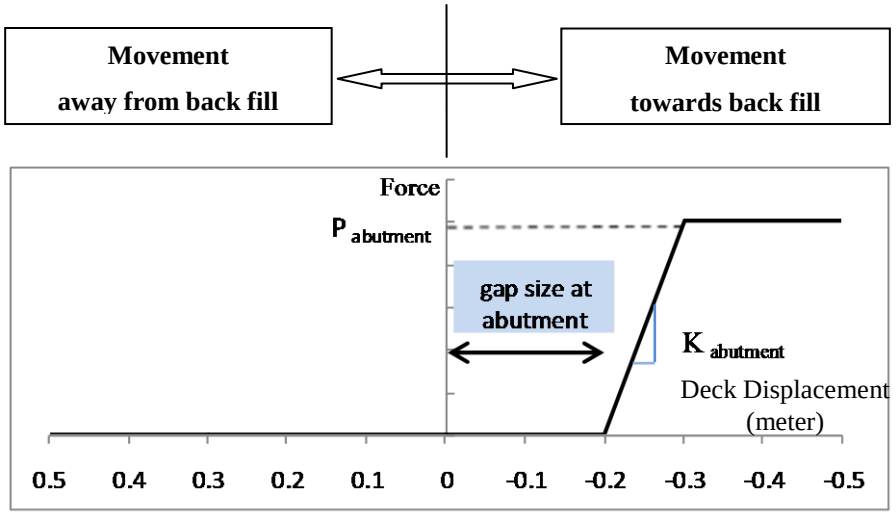

Fig. 3 Material model for "abutment-gap" system with effect of embankment, i.e., passive earth pressure behind back wall

4.2.3 Modeling of "buffer-gap-elastomeric bearings" system at piers

Bridge piers are modeled as elastic frame elements only for design purposes. However, in order to investigate the inelastic response under actual records, piers cross-sections are modeled using fiber elements and are divided into regular geometric configuration in the form of rectangular patches consisting of two distinct regions: (1) an unconfined region; and (2) a highly confined region inside the confinement reinforcement each represented by stress-strain properties that are a function of the different levels of confinement. For more details refer to Farag (2013). Elastomeric bearings are modeled with elastic springs in the horizontal direction similar to what has been followed for bearings on abutments' shelf. On the other hand, the seismic buffers at piers are considered in the current research via the two opposite vertical sides of the inverted web of the cap beam. These buffers are modeled by nonlinear horizontal springs, mounted in parallel with the elastic springs modeling the elastomeric bearings (refer to Figs. 4 and 5). These nonlinear springs (or so-called nonlinear gap elements in OpenSees library) are assigned zero stiffness for the negative displacements (i.e., tension, or deck moving away from the adjacent face of the cap beam), and for positive displacements (i.e., compression, or deck moving toward the adjacent face of the cap beam) up to the size of gap, d_g left between the end of precast beams and adjacent face of the inverted cap beam web. For positive displacements of the deck with values supposedly greater than d_g, the stiffness is considered practically infinite. As a result, a buffer of this form is activated only if the deck is moving towards the cap beam and the relative displacement of the deck relative to the pier top (i.e., the shear deformation within the bearings) becomes equal to d_g. Before this locking situation the system behaves nearly with the shear stiffness of the elastomeric bearings only. Or, to be more specific, the equivalent stiffness of the supporting system before locking situation is that of two springs in series: one of them corresponds to the elastomeric bearings themselves deforming in transverse shear mode, while the other corresponds to the pier lateral stiffness. The combined stiffness is hence less than the least of the two values which is simply that of the elastomeric bearings for most practical cases and most common piers height.

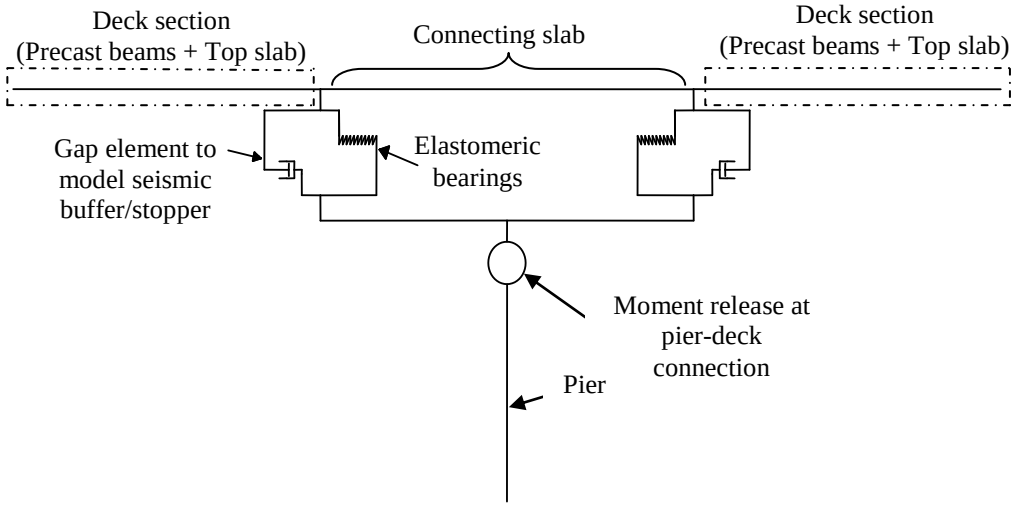

Fig. 4 Connection between pier top and bridge deck to model "buffer-gap-elastomeric bearings" system at top of piers

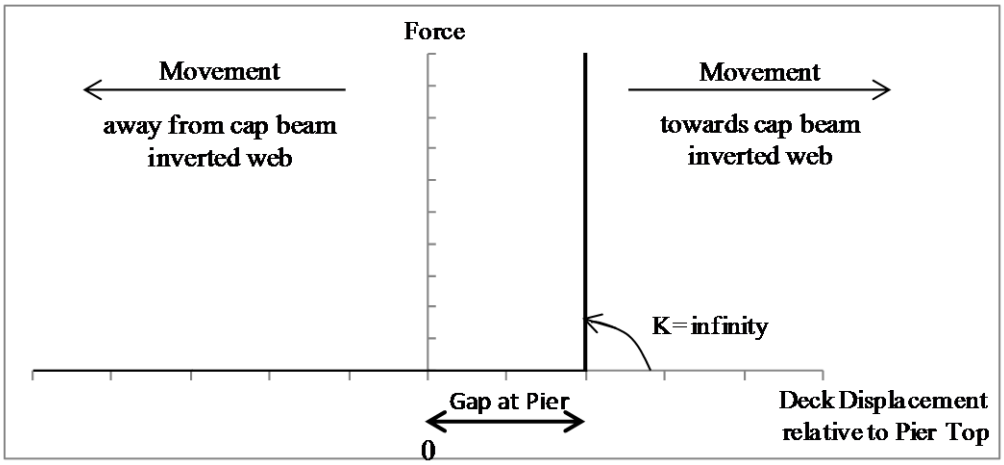

Fig. 5 Force-displacement schematic relation for the non-linear spring (i.e., gap element in OpenSees) modeling the seismic buffer at top of piers

To conclude, after engagement of buffers as a result of a large stroke of a given seismic event, the "buffer-gap-elastomeric bearings" system (with the bearings and buffer being two springs in parallel) has in the computational model an additive, and thus infinite, stiffness that is linked in series to the then much lower stiffness of the pier leading to an equivalent lateral stiffness for the system that is approximately equal to that of the pier. Note that if the two spans supported by the same pier are moving in the same direction, only the "buffer-gap-elastomeric bearings" system at the near side of the inverted web of the cap beam facing the deck movement is engaged while the "buffer-gap-elastomeric bearings" system at the far side of the inverted web of the cap beam is not activated. The stiffness of the latter is therefore only that of the elastic elastomeric bearings moving in an opening mode away from the cap beam inverted web.

4.2.4 Modeling of damping

Rayleigh (viscous) stiffness-proportional damping based on the tangent stiffness is considered in the case study bridge model, i.e., $[C]=\beta[K]$, where $[C]$ is the damping matrix, $[K]$ is the tangent stiffness matrix and β is the damping coefficient. Collapse capacity detected based on (tangent) stiffness-proportional damping assumption is generally less than that based on mass-proportional damping assumption (Ibarra and Krawinkler 2005); and hence the former assumption in modeling damping is at the conservative side from a design perspective and is accordingly adopted in the present research. β is computed and updated at each time step throughout the integration process of the equation of motion in order to guarantee a constant 5% viscous damping ratio assigned to the fundamental period of vibration all through the analysis up to collapse. The 5% equivalent viscous damping ratio is deemed appropriate to model the response of simple low-damping elastomeric bearings of the type used in this research as per EN 1998-2 (2005) - Cl. 7.5.1(3). The damping of these bearings may be further assumed equal to the global viscous damping of the bridge structure itself (EN 1998-2 2005).

The stiffness matrix used to build up the stiffness-proportional damping matrix is a tangent stiffness matrix as stated above and the proportionality coefficient β is also based on tangent

stiffness as recommended by Charney (2008) to avoid artificial damping. The tangent stiffness matrix referred to herein is generated at the last committed step of analysis relative to the current integration step of the equation of motion as per the formulation in OpenSees. The use of a "tangent" stiffness matrix is preferred over the "initial" stiffness matrix in order to avoid artificial damping forces that may typically arise when rigid elements used to model gap openings - such as those encountered in the current research - or plastic hinges have abrupt and extreme changes in their state. Such artificial (large) forces may be unintentionally orders of magnitude greater than the actual strength of the element that resists the same deformations.

4.3 Various design schemes of the case study bridge

Dimensioning of the case-study bridge piers starts by pre-selecting cross-section dimensions to satisfy gravity design and appropriate slenderness ratios to avoid buckling problems. Consequently, a response spectrum analysis is performed for the bridge in the longitudinal direction under the effect of a response spectrum (Type 1) constructed according to EN 1998-1 (2005) for ground accelerations, a_g, of 0.3 g and 0.15 g (considered to represent "moderate to high" and "low to moderate" seismic design demands, respectively), soil type B, and considering a high importance factor of 1.3. The analysis is performed for a two-dimensional design oriented model that is fully locked at all piers with non-sliding elastomeric bearings at abutments featuring a preset constant gap between precast beams end and abutment's back wall as outlined before. Seismic masses are calculated for the total dead load in addition to 20% of the live load. An effective inertia is used to model the bridge piers; it is taken as 50% of the pier gross inertia as per recommendations in Guirguis and Mehanny (2013) that were further supported by charts in Imbsen (2006) for typical bridge piers' cross-sections. The main concept followed herein in the piers design is to guarantee a factor of safety against flexure of exactly 1.0 relying on the generated "axial force-bending moment" interaction diagram for each pier, and the design values retrieved from the elastic response spectrum analysis after being reduced by the appropriate behavior value, q. Despite the fact that EN 1998-2 (2005) requires bridges with elastomeric bearings to be designed for q=1, it is allowed for these bridges when constructed with gaps and seismic buffers (that are activated during strong earthquakes and hence work like joints between the deck and the piers) to be designed for q values larger than 1 (Psycharis and Mageirou 2003).

Table 1 provides a summary of the piers reinforcement ratio for various design scenarios generated for the case study bridge. Different design scenarios have been generated for possible permutations of two different locations of the bridge associated with the two different design ground accelerations, a_g, mentioned above and for two codified values of q: namely, 3.5 for ductile behavior and 1.5 associated with limited ductility as per EN 1998-2 (2005). Two different heights of the bridge piers are also considered: H=7 m and H=14 m to represent short and high piers, respectively. The cross-section dimensions for the piers are nonetheless kept constant as 3.5×1.5 m measured in the transverse and longitudinal direction of the bridge, respectively, for both heights for the design scenarios with the design acceleration a_g=0.3 g, while they are taken as 3.5×1 m (again for both heights) for the design scenarios with a_g=0.15 g. These dimensions are believed to be appropriate from an aesthetical point of view as well as from a practical point of view satisfying a "safe for gravity" design as well as providing adequate slenderness ratio for the piers.

From Table 1, one could realize that only the design of the case study bridge subjected to a_g=0.15 g assuming ductile response (q=3.5) and with 14 m-high piers results in a reinforcement ratio, $\boldsymbol{\rho}$, of 0.094% which does not satisfy the minimum reinforcement ratio of 0.234% determined

Table 1 Summary of bridge piers reinforcement ratios (ρ) and fundamental period of vibration (T_1) of the "fully locked" design model for different considered design schemes and scenarios

	Design Ground Acceleration, a_g=0.3 g				**Design Ground Acceleration, a_g=0.15 g**			
	Ductile Response (q=3.5)		**Limited Ductility (q=1.5)**		**Ductile Response (q=3.5)**		**Limited Ductility (q=1.5)**	
	H=7 m	H=14 m	H=7 m	H=14 m	H=7 m	H=14 m	H=7 m	H=14 m
ρ(%)	1.37	0.81	3.78	2.15	0.51	0.094	1.73	0.47
T_1(sec)	0.577	1.4	0.577	1.4	0.95	1.65	0.95	1.65

as per EN 1992-1-1 (2004) - Cl. 9.5.2. However, in order for all design scenarios generated in the current research to represent realistic cases that do not violate code rules, it has been decided to increase this design-obtained reinforcement ratio of 0.094% to assume exactly the code minimum reinforcement ratio of 0.234% (determined for this particular case as per code requirement) for the investigation of the inelastic seismic response under the set of selected actual earthquake records.

5. Verifying proposed computational models via pushover analysis

A pushover analysis is carried out for validation of the proposed computational model. The bridge has been incrementally pushed in the longitudinal direction at its upper left point from left to right in the presence of the applicable gravity loads. According to the model outlined in the previous section, right abutment connection behaves in two phases. The first one is before the abutment's gap closure at which the connection stiffness is solely the bearing shear stiffness. The second phase is after the gap closure under the pushing load and then the connection equivalent stiffness suddenly climbs to the value of the abutment stiffness as shown in Fig. 6. On the other hand, the left abutment connection (behaving in a gap opening mode) only provokes the elastomeric bearings shear stiffness. Results of the pushover analysis should be disregarded after the deck displacement with respect to the left abutment shelf (i.e., the deformation within the non-sliding elastomeric bearings at this shelf) reaches a value of about three times the bearing thickness definitely referring to tearing of elastomer.

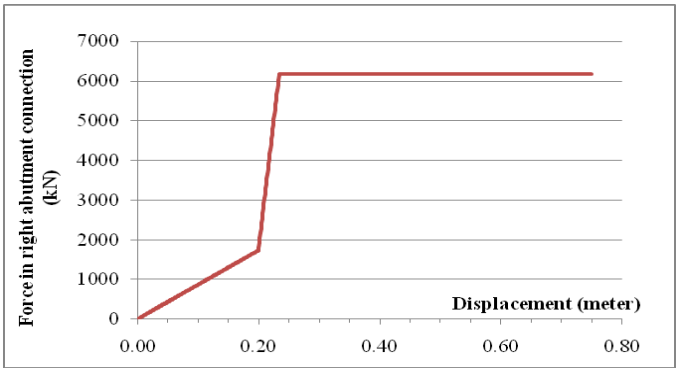

Fig. 6 Relation between the force developed in the right abutment connection and the deck displacement - Pushover Analysis

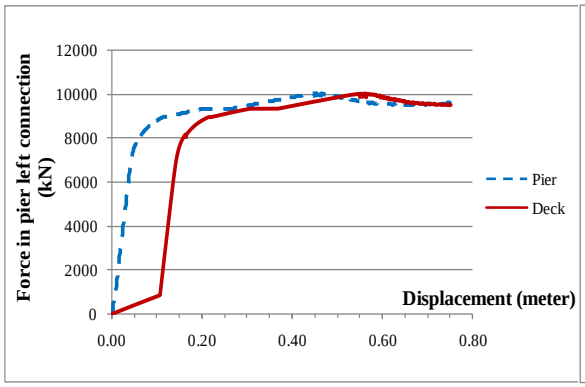

Fig. 7 Relation between deck displacement/pier top displacement and the force developed in the left connection at the pier top - Pushover Analysis

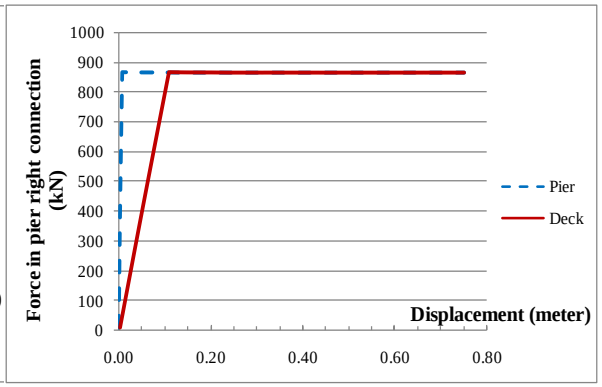

Fig. 8 Relation between deck displacement/pier top displacement and the force developed in the right connection at the pier top - Pushover Analysis

Figs. 7 and 8 show the response of the left and right connection elements at top of any of the two piers as a result of pushing the deck from left to right. It may be noticed that starting from the gap closure incident, the deck (i.e., point at top of bearing) and the top of pier (i.e., point at base of bearing) displace as one body under monotonic pushing in one direction until overall failure of the structure, be it either failure of the elastomeric bearings, off-seating of the deck from the left abutment's shelf or flexure failure in the reinforced concrete piers. Shown sample results are for the case study bridge with H=7 m, designed for ductile response (q=3.5) and a design ground acceleration a_g=0.3 g, and featuring 100 mm initial gap at piers and 200 mm at abutments.

6. Elements of incremental dynamic analysis for assessment up to collapse limit state

6.1 Actual ground records and adopted scaling technique

Seven recorded ground motions have been selected as follows: three recorded motions during the 1989 Loma Prieta earthquake, two recorded motions during the 1994 Northridge earthquake, one during the 1971 San Fernando earthquake and one during 1987 earthquake at Superstition Hills. Acceleration response spectrum curves for these seven real ground records are shown in Fig. 9. The records are taken out from the large database of records gathered in Medina (2002) and are originally extracted from the PEER (Pacific Earthquake Engineering Center) ground motion database. For specific details of selected ground motion records one may be referred to Farag (2013) and Medina (2002). These records were extensively used in several other earlier studies (e.g., Mackie and Stojadinović 2005, Mehanny and Ayoub 2008, Mehanny 2009).

Scaling of these actual records at progressively increasing seismic demand to generate incremental dynamic analysis curves up to collapse limit state has been implemented through successively increasing Sa levels determined from each record-specific response spectrum at the numeric value of T1. T1 is the fundamental period retrieved from the design model that is fully locked and using cracked inertia (50% gross inertia) for piers and un-cracked inertia for deck. We do not say that Sa(T1) represents for sure an optimal Intensity Measure (IM), but at least it is a good-potential candidate IM that is commonly used and that is convenient and practical to deal

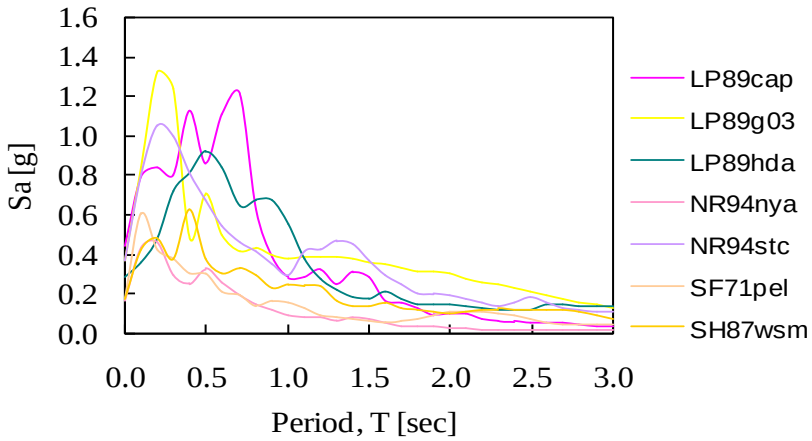

Fig.9 Acceleration response spectrum curves for the seven selected ground records.

with since it is based herein on a single reference value of the period (namely, T1) irrespective of the analysis model used in the inelastic time history analysis (i.e., irrespective of the model being fully locked or with a starting gap, and irrelevant of the size of this original gap). Moreover, as an ongoing research effort, the authors are looking into better (i.e., optimal - if any) IMs than Sa(T1) for this problem of the "buffer-gap-elastomeric bearings" system - either by referring to other value(s) of the period of vibration or by adopting other IMs such as the spectral velocity Sv, etc. - in order to display less record-to-record variability of (and minimize the scatter in) the engineering demand parameters of interest conditioned on this optimal IM.

6.2 Manipulation of recorded/monitored demand parameters

After performing incremental dynamic analysis up to failure for each given design scheme of the case study bridge for various discrete initial gap sizes intentionally introduced at piers and abutments, three main seismic demand parameters are monitored and hence manipulated to assess the inelastic seismic response of the original design but in presence of an actual "buffer-gap-elastomeric bearings" system. To recall, the design has been performed based on a "Fully Locked (FL)" model. The first parameter recorded is $S_a\,(T1)_{failure}$ which is the value of the spectral acceleration at failure limit state under a specific earthquake record, where T1 as previously stated is always that of the FL design model (i.e., with zero initial gap at all piers). The second parameter is Φ_{max} which is the maximum value of curvature demand at the base of pier associated with the design level earthquake (i.e., the actual earthquake record scaled up to the same value of the code "elastic" response spectrum). The third and last parameter is M_{max} which is the maximum value of bending moment at the base section of pier again associated with the design level earthquake as for Φ_{max}.

At the collapse (i.e., failure) limit state, a dimensionless quantity R_c is introduced

$$R_c = \frac{S_a(T_1)_{failure,Gap}}{S_a(T_1)_{failure,Locked}} \tag{1}$$

where $S_a(T1)_{failure,Gap}$ is the spectral acceleration of the actual record scaled up to the level that

causes failure of the bridge modeled with an actual "buffer-gap-elastomeric bearings" system; while $S_a(T1)_{failure,Locked}$ is that value associated with failure of the bridge modeled as FL since the first instant of applying the earthquake record. If $R_c>1$ for a given nominal actual initial gap size introduced (either intentionally or unintentionally) at piers in a bridge originally designed for the FL condition, the design technique that has been adopted herein based on the FL condition is hence conservative with respect to collapse limit state since it provides a larger capacity of the actual (as-built) bridge. Conversely, if $R_c<1$ the design technique based on the FL condition is accordingly not suitable for that bridge equipped on-site with actual initial gap at piers.

At the design level earthquake, i.e., at $S_a(T1)$ equal to the value retrieved from code elastic response spectrum (with q=1) used for design purposes, two other dimensionless seismic design parameters are introduced, namely: $R_d(\Phi)$ and $R_d(M)$

$$R_d(\Phi \text{ or } M) = \frac{\Phi_{\text{max, Gap}}}{\Phi_{\text{max, Locked}}} \text{ or } \frac{M_{\text{max, Gap}}}{M_{\text{max, locked}}} \tag{2}$$

$R_d(\Phi)<1$ or $R_d(M)<1$ means that an actual initial gap on site for a bridge designed for the FL condition will reduce the anticipated seismic demand (in terms of curvature and hence bending moment at base of pier) under actual earthquakes corresponding to the design level earthquake. It is worth highlighting that when computing $R_d(\Phi)$ *at the design level earthquake*, an average (of all seven records) monitored Φ_{max} is first calculated and then $R_d(\Phi)$ is computed only once as per Eq. 2 based on relevant values of this average Φ_{max} in the numerator and the denominator of the equation; we thus simply compute "quotient of average $\Phi_{max's}$". This should be similarly applied when estimating $R_d(M)$. The rationale behind this approach is that we always design as per code requirements for the average demand of several records (seven or more). Conversely, R_c is first calculated per Eq. (1) for each record to get actual reserve capacity *at failure* for each record separately, and then an average (i.e., "average of the quotient in Eq. (1)") R_c for all seven records is computed for each design scheme.

6.3 Adopted failure criteria for the case study bridge

Failure of the bridge in the present research is assumed to take place at whichever of the following occurs first: (1) curvature demand at the base cross-section of pier reaches Φ_R which is the ultimate curvature resistance (determined via section fiber analysis) corresponding to the pier's maximum moment resistance M_R (according to Guirguis and Mehanny 2013, SCDOT 2008); hence, only flexure failure of the pier was considered while assuming that shear failure and buckling were not expected to occur; or (2) deck displacement reaches a maximum value of 100 cm (for the 0.3 g design models) or 70 cm (for the 0.15 g design models). If deck displacement exceeds these values, the deck falls off the abutment seat after bearing failure/tearing. It is worth noting that for the present research the first failure criterion always prevails.

There is another failure criterion worth discussing and investigating. It is manifested by a failure mode entailing breaking and tearing of the non-sliding elastomeric bearings at abutments when the deck displacement reaches a maximum value of three times the elastomer thickness t_b (i.e., for 0.3 g design, t_b=150 mm then $3t_b$=450 mm, and for 0.15 g design, t_b=100 mm then $3t_b$=300 mm). This lateral deformation of $3t_b$ within the bearing assumed herein to demarcate "full" tearing of the elastomeric bearing is selected based on scattered information gathered from experimental and analytical results in the literature as pinpointed in a previous section. However,

this criterion is not strictly marking a collapse state of the bridge as a whole. Total bridge failure will not happen since there has not been yet an off-seating of the deck from the bearings resting on the abutments' shelves; maximum deck displacement has not yet exceeded off-seating limiting values identified above. Hence, tearing of bearings without off-seating may be considered a "weak" mode of failure that could be restored by bearing replacement.

7. Results and discussions of the incremental dynamic analysis

This section is dedicated to present and discuss the results of the time history inelastic analysis of different design schemes both at the design demand level and at collapse limit state. Given results are averaged over all seven selected ground records for different investigated as-built (initial) gap sizes at piers ranging from zero (i.e., completely engaged seismic buffers) up to a maximum gap that is three quarters the initial gap at abutments. It is to be noted that the initial as-built gaps at abutments are 200 and 100 mm for the bridge schemes designed for a_g=0.3 g and 0.15 g, respectively. These values are in line with gathered data from the literature (Yilmaz 2008), as well as extensive design experience of the second author with real precast beam bridges located in high and moderate seismic zones (particularly in Turkey and Algeria).

7.1 Bridge schemes designed for a_g=0.3 g with non-sliding bearings at piers and abutments

Referring to Fig. 10(a), the bridge scheme with short piers (H=7 m) designed for ductile behavior (q=3.5) shows different behavior - averaged over the seven selected records - compared to the case designed for limited ductility (q=1.5). For the former, the reserve capacity against failure (relative to the case with FL condition) - on average - drops down at an actual starting gap size of 50 mm (R_c=0.76), then increases gradually with the increase of gap size. The value of R_c is however still slightly less than 1.0 (namely 0.96) for an actual starting gap size of 100 mm and it only marginally exceeds 1.0 for the case of as-built initial (quite large) gap size at piers of 150 mm. Hence, the design approach based on the FL condition is generally not suitable and does not improve the reserve collapse capacity in the presence of actual reasonable (50 to 100 mm) gaps on site while it provokes only 7% reserve capacity over the FL condition with 150 mm initial gap at piers. On the other hand, the limited ductility design (q=1.5) provides reserve capacity at failure relative to the FL bridge version for all investigated actual initial gaps at piers, reaching a maximum of 20% overstrength for the largest initial gap of 150 mm (namely, three quarters the initial gap at abutments).

Similarly, referring to Figs. 10(b) and 10(c), it is observed that at the design level earthquake $R_d(M)$ and $R_d(\Phi)$ show nearly same response for the two bridge schemes with 7 m long piers designed for either q=1.5 or q=3.5 except for an actual starting gap of 50 mm. $R_d(M)$ and $R_d(\Phi)$ score larger values at gap=50 mm relative to "zero" gap condition then decrease for larger gaps (100 and 150 mm) for the case designed for q=1.5, while they score continuously decreasing values for all investigated initial gap sizes at piers relative to the zero gap condition for the bridge scheme designed for ductile behavior (q=3.5).

It is nonetheless worth noting that all failure incidents monitored for the bridge schemes featuring short piers (H=7 m) and designed either for q=1.5 or 3.5 are pier flexure failure and not bearing failure (either tearing of elastomer or deck/bearing off-seating at abutment). It has been

further observed that for all seven considered earthquakes the gap at piers is closed at the failure level, while at the design level earthquake the as-built initial gap at piers is closed for some records while it is still open for other records, thus revealing a non-engagement of the seismic buffers for these records at the design level earthquake.

The bridge scheme with long piers (H=14 m) and designed for limited ductility (q=1.5) shows that, while the actual initial gap at piers increases, the reserve capacity against failure relative to the FL condition first slightly drops down (R_c=0.96) for the scheme featuring an initial (fairly small) gap size of 50 mm then increases to become 1.1 (i.e., scoring a 10% increase in bridge capacity) for the case of actual initial gap size of 100 mm; refer to Fig. 10(a). This value for R_c remains constant for the other investigated case with larger initial gap size of 150 mm. Conversely, regarding the other case designed for q=3.5, the reserve capacity against failure is nearly zero and is further constant for all investigated cases with various actual initial gap sizes at piers. It is further worth noting that the failure for cases with moderate to large actual initial gaps (100 and 150 mm) at piers has happened while the gap is still open, i.e., with no engagement of the seismic buffers. This observed response is expected by intuition since the "buffer-gap-elastomeric bearings" system is anticipated to be less efficient in improving the seismic response of bridges when these bridges feature fairly long piers and are further originally designed for ductile behavior; the stiffness of such piers is generally relatively smaller as a result of dimensioning them for q=3.5, and hence the system is globally more flexible.

One further important observation to be noted when referring to recorded results of H=14 m bridge schemes is that elastomeric bearing failure at abutments has occurred for almost all records (i.e., relative displacement between deck and abutment has exceeded the limiting bearing failure value which is three times the elastomer thickness). Bearing failure according to this definition occurs at average (over the seven records) S_a(T1) values lower than those reported in Table 2 defining flexure failure of reinforced concrete piers. For instance, for the bridge scheme with H=14 m and q=1.5, S_a(T1) values demarking failure of non-sliding bearings on abutment's shelf, averaged over all records, are 2.97 g, 2.73 g, 2.78 g and 2.63 g (i.e., lower than values associated with pier failure given in Table 2) for as-built initial gap sizes at piers of 0, 50, 100 and 150 mm, respectively. However, this bearing failure criterion is not strictly marking a collapse state as outlined before since there has not been yet an off-seating from the abutments' shelves. Therefore, it has been decided to further scale up seismic records in order to monitor real collapse in terms of pier flexure failure which has resulted in the values of $S_a(\text{T1})_{\text{failure}}$ reported in Table 2.

On the other hand, from a design point of view, at the design level earthquake as noticed from Figs. 10(b) and 10(c), $R_d(\Phi)$ and $R_d(M)$ score values less than 1.0 and further decrease as the actual initial gap size increases except for the bridge with 14 m long piers designed for limited ductility (q=1.5) but featuring an actual initial gap size=50 mm when constructed. This response is very similar to that of the bridge with H=7 m and also designed for limited ductility.

Finally, referring to Table 2, as expected by intuition, bridge schemes with either short or long piers designed assuming limited ductility (q=1.5) have - on average - failed at $S_a(\text{T1})_{\text{failure}}$ levels greater than their equivalent schemes designed for ductile behavior (q=3.5). This occurs for all investigated actual initial gap sizes at piers. Such response is anticipated since the strength (as reflected herein by the amount of reinforcing steel in the piers cross-section) inherent with the q=1.5 design is much larger than that for the q=3.5 design.

7.2 Bridge schemes designed for a_g=0.15 g with non-sliding bearings at piers and abutments

For the bridge scheme with short piers (H=7 m) and designed for q=3.5, and referring to Fig. 11(a), it has been noted that while the as-built initial gap at piers increases, the reserve capacity against failure of the bridge - originally designed based on a FL condition model - relative to that of the bridge built with zero gap condition at piers first drops down for the scheme with initial as-built gap size of 25 mm (R_c is less than one), then increases to an R_c of 1.21 for the bridge schemes with initial as-built gap sizes of 50 and 75 mm at piers. This means that if a particular bridge is designed based on the FL model for a ductile behavior (q=3.5) then constructed with an initial gap size at piers of 50 or 75 mm, the reserve capacity at failure will be 21% greater than if the same bridge (as designed) is built with zero gap at all piers.

On the other hand, at the design level earthquake - refer to Table 3 - for the q=3.5 design, both Φ_{max} and M_{max} (averaged over all records) are reduced as the actual initial gap size at piers increases. It is further noted that for the current investigated case study bridge (designed for a_g=0.15 g, H=7 m and q=3.5), the initial as-built gaps at piers remain open at the design level earthquake for actual initial gap sizes of 50 and 75 mm.

It is also worth noting that all failure incidents that occurred for this bridge scheme with H=7 m and designed for q=1.5 or 3.5 represent pier failure and not tearing of the elastomeric bearings or off-seating from the abutments. However, it is also worth reporting that for the q=3.5 design -both at the design level earthquake and at the failure level earthquake - the as-built initial gap at piers is closed for some particular scenarios (in terms of actual initial gap size at piers and associated specific earthquake records) while it remains open for other cases.

On the other hand, the investigated bridge schemes with H=14 m and designed for q=1.5 or 3.5 undergo bearing failure (i.e., tearing/breaking of the elastomeric non-sliding bearings) at abutments for almost all records before pier flexure failure except for one out of the seven records; refer to Farag (2013) for details. Such bearing failure occurs at S_a(T1) values lower than those reported in Table 3 defining flexure failure of reinforced concrete piers; namely, S_a(T1) values demarking failure of non-sliding bearings on abutments shelves, averaged over all seven records, are 1.25 g, 1.28 g, 1.28 g and 1.28 g for as-built initial gap sizes at piers of 0, 25, 50 and 75 mm, respectively. However, no off-seating of the deck from the abutment's shelf has been reported. Therefore, it has been decided to further scale up seismic records in order to monitor real collapse in terms of pier failure which has resulted in the values of $S_a(T1)_{failure}$ reported in Table 3. It may be also noticed that for all bridge schemes with H=14 m designed for q=1.5 or 3.5, the as-built initial gap at piers does not affect the reserve capacity of the bridge against failure because of the fairly relatively low stiffness of the pier which renders the overall bridge system more flexible. Hence, for these bridges with quite long piers and designed in low to moderate seismic zones (i.e., a_g=0.15 g), the "gap-buffer-elastomeric bearings" system may not be that efficient in reducing the seismic design demand or improving the reserve capacity of the bridge against failure. Consequently, it may be expected as is also clear from Figs. 11(b) and 11(c) that at the design level earthquake $R_d(\Phi)$ and $R_d(M)$ remain constant with a value that is practically 1.0 as the actual initial gap size at piers assume various values (ranging from zero, i.e., no gap at piers up to a value of 75 mm which is three quarters the gap at abutments).

To conclude, it may be noted that for all bridge schemes designed in low to moderate seismic zones (a_g=0.15 g), the as-built initial gap at piers (and especially the case of large gap sizes that are ≥1/2 the as-built gap at abutments) does not practically affect the reserve capacity of the bridge against failure for bridges featuring long piers (i.e., H=14 m). This is mainly because of the fairly relatively low stiffness of the pier (its stiffness is very comparable to that of the system of elastomeric bearings resting on its top) which renders the overall bridge system quite flexible. To

the contrary, the "gap-buffer-elastomeric bearings" system is more effective for the bridge schemes where there is a large difference between the stiffness of the elastomeric bearings and that of their supporting (much stiffer) reinforced concrete squat piers (like is the case for the H=7 m schemes). Such effectiveness is even amplified - both at the design level and at the collapse level - for the case of larger initial as-built gap sizes at piers.

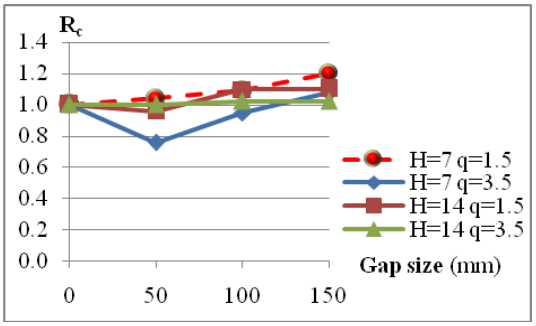

Fig. 10(a) Relation between R_c(averaged over pre-selected records) and as-built initial gap size at piers for bridge schemes with H=7 m & H=14 m, q=1.5 & q=3.5, designed for a_g=0.3 g

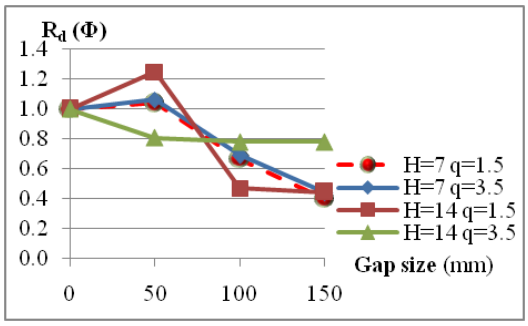

Fig. 10(b) Relation between R_d(Φ) and actual initial gap size at piers for bridge schemes with H=7 m & H=14 m, q=1.5 & q=3.5, designed for a_g=0.3 g

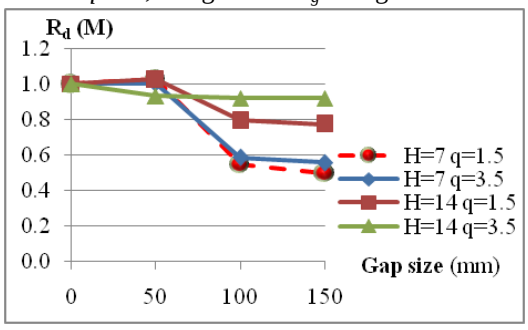

Fig. 10(c) Relation between R_d(M) and as-built initial gap size at piers for bridge schemes with H=7 m & H=14 m, q=1.5 & q=3.5, designed for a_g=0.3 g

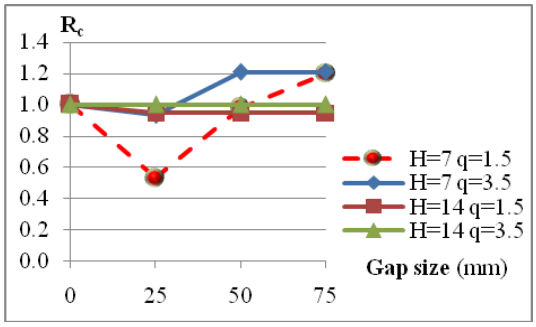

Fig. 11(a) Relation between R_c(averaged over pre-selected records) and as-built initial gap size at piers for bridge schemes with H=7 m & H=14 m, q=1.5 & q=3.5, designed for a_g=0.15 g

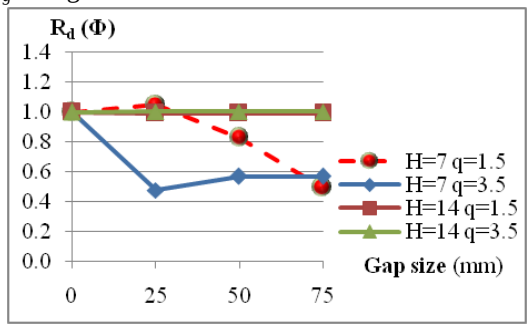

Fig. 11(b) Relation between R_d(Φ) and actual initial gap size at piers for bridge schemes with H=7 m & H=14 m, q=1.5 & q=3.5, designed for a_g=0.15 g

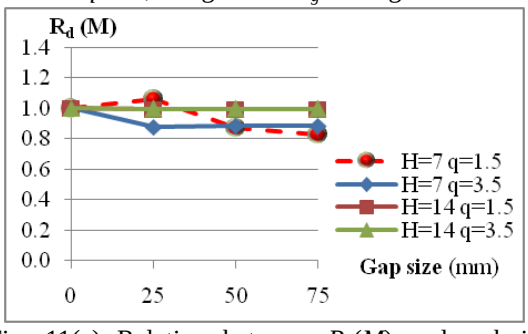

Fig. 11(c) Relation between R_d(M) and as-built initial gap size at piers for bridge schemes with H=7 m & H=14 m, q=1.5 & q=3.5, designed for a_g=0.15g

Table 2 Results - averaged over all seven ground records - for bridge schemes designed for moderate to high seismic demands, a_g=0.3 g

Gap Size[**] **(mm)**	**Limited Ductility Design, *q*=1.5**			**Ductile Design, *q*=3.5**		
	$S_a(T_1)_{failure}$ **(g)**	Φ_{max}[*] **(1/m)**	M_{max}[*] **(kN.m)**	$S_a(T_1)_{failure}$ **(g)**	Φ_{max}[*] **(1/m)**	M_{max}[*] **(kN.m)**
Schemes with Short Piers, H=7 m						
0	3.41	0.0099	53070	3.21	0.0205	26160
50	3.84	0.0103	54540	2.44	0.0188	24760
100	3.92	0.0066	29130	2.93	0.0008	9770
150	4.16	0.0040	26450	3.44	0.0008	9770
Schemes with Long Piers, H=14 m						
0	4.51	0.0042	29220	2.78	0.0075	15390
50	3.96	0.0052	29900	2.71	0.0060	14320
100	4.85	0.0020	23170	2.74	0.0058	14160
150	4.81	0.0019	22610	2.74	0.0058	14160

[*]Φ_{max} and M_{max} are maximum values throughout time histories monitored at base of piers, averaged over all seven records and associated with the design level earthquake
[**]Initial actual gap size at piers taking into account that initial gap at abutments is 200 mm

Table 3 Results - averaged over all seven ground records - for bridge schemes designed for low to moderate seismic demands, a_g=0.15 g

Gap Size[**] **(mm)**	**Limited Ductility Design, *q*=1.5**			**Ductile Design, *q*=3.5**		
	$S_a(T_1)_{failure}$ **(g)**	Φ_{max}[*] **(1/m)**	M_{max}[*] **(kN.m)**	$S_a(T_1)_{failure}$ **(g)**	Φ_{max}[*] **(1/m)**	M_{max}[*] **(kN.m)**
Schemes with Short Piers, H=7 m						
0	1.55	0.0054	11030	0.90	0.0246	6830
25	0.90	0.0057	11690	0.85	0.0117	5990
50	1.49	0.0045	9610	1.10	0.0139	6040
75	1.76	0.0027	9150	1.10	0.0139	6040
Schemes with Long Piers, H=14 m						
0	1.80	0.0019	4500	1.37	0.0022	398
25	1.74	0.0018	4460	1.39	0.0022	396
50	1.74	0.0018	4460	1.39	0.0022	396
75	1.74	0.0018	4460	1.39	0.0022	396

[*]Φ_{max} and M_{max} are maximum values throughout time histories monitored at base of piers, averaged over all seven records and associated with the design level earthquake
[**] Initial actual gap size at piers taking into account that initial gap at abutments is 100 mm

8. Conclusions

Main conclusions of the present research are summarized as follows:

8.1 Bridge schemes designed for moderate to high seismic demands with a_g=0.3 g

For schemes with short piers: For bridges designed for limited ductility behavior as per EC8, the reserve capacity at failure is larger than 1.0 for all investigated gap schemes (i.e., initial gap size at piers ranging from a quarter to three quarters that at abutment). On the other hand, for bridges designed for ductile behavior then constructed with a given nominal actual initial gap, a large gap at piers which is three quarters the as-built gap at abutments is recommended to improve the capacity against collapse for this ductile design.

For schemes with long piers: The design with limited ductility shows that, while the actual initial gap at piers increases, the reserve capacity against failure relative to the designed fully locked condition first slightly drops down for the scheme featuring an initial (fairly small) gap size that is equal to quarter of the as-built gap at abutments, then climbs up to score a 10% increase in bridge capacity against collapse leading to some overstrength for the case of actual initial gap size at piers that is half of the initial gap size at abutments. This increase remains constant for the other investigated case with larger initial gap size at piers that is 3/4 the gap at abutment. On the other hand, when q=3.5 the reserve capacity against failure is not only nearly zero but is further also constant for all investigated cases with various actual initial gap sizes at piers. It is further worth noting that the failure for cases with moderate to large actual initial gaps at piers (namely, 1/2 and 3/4 those at abutments) has happened while the gap is still open, i.e., with no engagement of the seismic buffers. This observed response is expected by intuition since the "buffer-gap-elastomeric bearings" system is anticipated to be less efficient in improving the seismic response of investigated bridges when these bridges feature fairly long piers and are in addition originally designed for ductile behavior.

8.2 Bridge schemes designed for low to moderate seismic demands with a_g=0.15 g

It has been noted that the as-built initial gap at piers (and especially large gaps that are ≥1/2 as-built gap at abutments) does not practically affect the reserve capacity of the bridge against failure for bridges featuring long piers. This is mainly because of the fairly relatively low stiffness of the pier (its stiffness is very comparable to the system of elastomeric bearings resting on its top) which renders the overall bridge system quite flexible and less reactive to the isolation mechanism introduced by the elastomeric bearings. Hence, for these bridges with long piers, the "buffer-gap-elastomeric bearings" system may not be that efficient in reducing the seismic design demand or improving the reserve capacity of the bridge against failure. To the contrary, the "buffer-gap-elastomeric bearings" system is more effective for the bridge schemes where there is a large difference between the stiffness of the elastomeric bearings and that of their supporting (much stiffer) reinforced concrete squat piers such as for the H=7 m schemes. Such effectiveness is even amplified - both at the design level and at the collapse level earthquakes - for the case of larger initial as-built gap sizes at piers.

It is nonetheless important to realize that piers' behavior (and hence global bridge failure) in the present research is exclusively governed by flexure, while shear failure and buckling are currently not controlling, and that soil-structure interaction at piers foundation is not considered in the seismic analysis. Extrapolation of the results presented herein to other bridge geometric configurations (including skew and curved layouts) shall be the subject of a similar effort before such results are either applied or denied. It is also worth reporting that some additional schemes of the case study bridges - often encountered in practice - will be the subject of another publication

by the authors due to space limitations. These scenarios encompass: (a) bridges with sliding elastomeric bearings at abutments; (b) bridges using lower elastomeric bearing stiffness at piers and at abutments; and (c) bridges with different gap sizes at left and right sides of each pier due to construction imperfections and thermal deformations of the deck.

Acknowledgments

The research reported here was supported by the European Union Project PIRSES-GA-2010-269222: Analysis and Design of Earthquake Resistant Structures (ADERS) of the FP7-PEOPLE-2010-IRSES, Marie Curie Actions. This support is gratefully acknowledged by the authors.

References

AASHTO (2002), *Standard Specifications for Highway Bridges*, 17th Edition, Washington, DC., USA.

Ayoub, E.F. and Helmy, G. (2000), "Modeling of the elastomeric bearings for the seismic analysis of precast girder bridges", *Bridge Engineering Conference*, Sharm-ElSheikh, Sinai, Egypt.

Aviram, A., Mackie, K.R. and Stojadinovic, B. (2008), "Effect of abutment modeling on the seismic response of bridge structures", *Earthq. Eng. Eng. Vib*., **7**(4), 395-402.

Bandyopadhyay, N., Ghoshal, A. and Sengupta, A. (2010), "Relevance of bearings and expansion joints - case studies for indeterminate bridges", *IABSE-JSCE Joint Conference on Advances in Bridge Engineering-II*, Dhaka, Bangladesh.

Buckle, I.G., Constantinou, M.C., Dicleli, M. and Ghasemi H. (2006), "Seismic isolation of highway bridges", *Special Report MCEER-06-SP07*, Buffalo, NY.

California Department of Transportation (CalTrans) (1999), "Bridge Memo to Designers(20-1)", *Seismic Design Methodology, California Department of Transportation*, Sacramento, CA.

Caltrans (SDC) (2009), *Seismic Design Criteria*, Version 1.5.

Charney, F.A. (2008), "Unintended consequences of modeling damping in structures", *J. Struct. Eng.*, ASCE, **134**(4), 581-592.

DesRoches, R. and Muthukumar, S. (2002), "Effect of pounding and restrainers on seismic response of multi-frame bridges", *J. Struct. Eng.*, ASCE, **128**(7), 860-869.

Dicleli, M. (2002), "Seismic design of lifeline bridge using hybrid seismic isolation", *J. Bridge Eng.*, ASCE, **7**(2), 94-103.

EN 1992-1-1 Eurocode 2 (2004), *Design of Concrete Structures. Part 1-1: General Rules and Rules for Buildings*, *ComitéEuropéen de Normalisation*, Brussels, Belgium.

EN 1992-2 Eurocode 2 (2005), *Design of Concrete Structures. Part 2: Concrete Bridges – Design and Detailing Rules*, *ComitéEuropéen de Normalisation*, Brussels, Belgium.

EN 1998-1 Eurocode 8 (2005), *Design of Structures for Earthquake Resistance. Part 1: General Rules, Seismic Actions and Rules for Buildings*, *ComitéEuropéen de Normalisation*, Brussels, Belgium.

EN 1998-2 Eurocode 8 (2005), *Design of Structures for Earthquake Resistance, Part 2: Bridges*, *ComitéEuropéen de Normalisation*, Brussels, Belgium.

Farag, M.M.N. (2013), "Inelastic seismic response of bridges with a buffer-gap-elastomeric bearing system", MSc. Thesis, Faculty of Engineering, Cairo University.

Guirguis, J.E.B. and Mehanny, S.S.F. (2013), "Evaluating codes criteria for regular seismic behavior of continuous concrete box girder bridges with unequal height piers", *J. Bridge Eng.*, ASCE, **18**(6), 486-498.

Hindi, R. and Dicleli, M. (2006), "Effect of modifying bearing fixities on the seismic response of short- to medium-length bridges with heavy substructures", *Earthq. Spectra*, **22**(1), 65-84.

Ibarra, L.F. and Krawinkler, H. (2005), "Global collapse of frame structures under seismic excitations", *Blume Center Report No. 152*, School of Civil and Environmental Engineering, Stanford University, CA.

Imbsen, R.A. (2006), "Recommended LRFD guidelines for the seismic design of highway bridges", *prepared as part of NCHRP*, Project 20-07, Task 193, TRB.

Japan Road Association (JRA) (1997), *Manual for seismic design of highway bridges*, Tokyo, Japan.

Japan Road Association (JRA) (2002), "Chapter 1 seismic design specifications for highway bridges", *International Institute of Seismology and Earthquake Engineering*, Tokyo, Japan.

Karsan, I.D. and Jirsa, J.O. (1969), "Behavior of concrete under compressive loading", *J. Struct. Div*., ASCE, **95**(ST12), 2543-2563.

Konstantinidis, D., Kelly, J.M. and Makris, N. (2009), "Experimental investigation on the seismic response of bridge bearings", *3rd International Conference on Advances in Experimental Structural Engineering*, San Francisco, CA.

Kunde, M.C. and Jangid, R.S. (2006), "Effects of pier and deck flexibility on the seismic response of isolated bridges", *J. Bridge Eng*., ASCE, **11**(1), 109-121.

Mackie, K.R. and Stojadinović, B. (2005), "Fragility basis for California highway overpass bridge seismic decision making", *PEER Report 2005/02*, University of California, Berkeley, CA, USA.

Manos, G.C., Mitoulis, S.A. and Sextos, A.G. (2011), "Preliminary design of seismically isolated R/C highway overpasses - features of relevant software and experimental testing of elastomeric bearings", COMPDYN 2011, *III ECCOMAS Thematic Conference on Computational Methods in Structural Dynamics and Earthquake Engineering*, Corfu, Greece.

Medina, R. (2002), "Seismic demands for non-deteriorating frame structures and their dependence on ground motions", Ph.D. Thesis, Department of Civil and Environmental Engineering, Stanford University, CA, USA.

Mehanny, S.S.F. and Ayoub, A.S. (2008), "Variability in inelastic displacement demands: Uncertainty in system parameters versus randomness in ground records", *Eng. Struct*., **30**(4), 1002-1013.

Mehanny, S.S.F. (2009), "A broad-range power-law form scalar-based seismic intensity measure", *Eng. Struct.*, **31**(7), 1354-1368.

Mitoulis, S.A. (2013), "Bridges with fixities and bearings versus isolated sytems", *Proceedings of the 4th International Conference on Computational Methods in Structural Dynamics and Earthquake Engineering*, Kos Island, Greece.

Mitoulis, S.A. and Tegos, I.A. (2010), "Restrain of a seismically isolated bridge by external stoppers", *Bull. Earthq. Eng*., **8**(4), 973-993.

Monzon, E.V., Wei, C., Buckle, I.G. and Itani, A. (2012), "Seismic response of full and hybrid isolated curved bridges structures", *ASCE Congress*, Chicago, Illinois, USA.

OpenSees 2.0.0 [Computer software], Berkeley, CA, Pacific Earthqakes Engineering Response Center, University of California.

Psycharis, I.N. and Mageirou, G.E. (2003), "Parametric investigation of the inelastic seismic response of bridges with elastomeric bearings combined with stoppers", *fib Symposium on Concrete Structures in Seismic Regions*, Athens, Greece.

Scott, B.D., Park, R. and Priestley, M.J.N. (1982), "Stress-strain behavior of concrete confined by overlapping hoops at low and high strain rates", *ACI J.*, **79**(1), 13-27.

South Carolina Department of Transporation (SCDOT) (2008), "Seismic design specifications for highway bridges", version 2.0, SCDOT,Columbia, SC.

Stefanidou, S.P. and Kappos, A.J. (2013), "Optimum selection of retrofit measures for R/C bridges using fragility curves", *Proceeding of the 4th International Conference on Computational Methods in Structural Dynamics and Earthquake Engineering*, Kos Island, Greece.

Wang, K., Wei, H. and Li, Q. (2012), "Philosophies on seismic design of highway bridge with small or medium span", *Proceedings of 15th WCEE - World Conference on Earthquake Engineering*, Lisbon,

Portugal.
Yilmaz, T. (2008), "Seismic response of multi-span highway bridges with two-column reinforcement concrete bents including foundation and column flexibility", MSc. Thesis, Middle East Technical University, Turkey.

JL